

Synthesis, spectroscopic characterization, DNA interaction and biological activities of Mn(II), Co(II), Ni(II) and Cu(II) complexes with [(1H-1,2,4-triazole-3-ylimino)methyl]naphthalene-2-ol



Mohamed Gaber^a, Nadia A. El-Wakiel^{a,*}, Hoda El-Ghamry^{a,b}, Shaimaa K. Fathalla^a

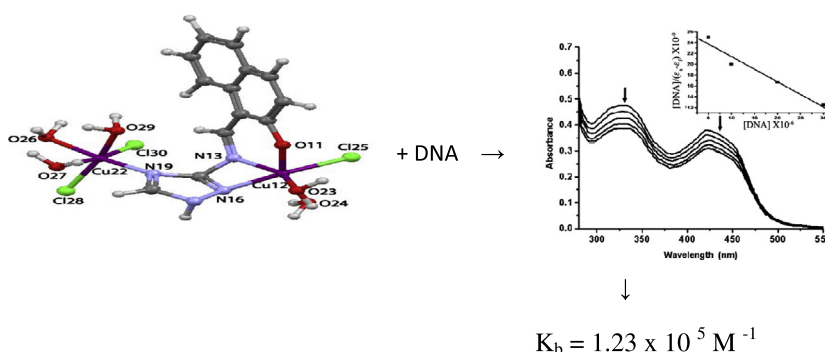
^a Chemistry Department, Faculty of Science, Tanta University, Tanta 31725, Egypt

^b Chemistry Department, Faculty of Applied Science, Umm Al-Qura University, Makkah, Saudi Arabia

HIGHLIGHTS

- Novel manganese (II), cobalt(II), nickel(II) and copper(II) complexes of [(1H-1,2,4-triazole-3-ylimino)methyl]naphthalene-2-ol were synthesized.
- The structures of the prepared complexes were elucidated.
- The binding mode of the metal complexes towards DNA were studied.
- The compounds were screened for antibacterial and antifungal activity indicating enhanced activity of ligand upon chelation.

GRAPHICAL ABSTRACT



ARTICLE INFO

Article history:

Received 9 May 2014

Received in revised form 21 June 2014

Accepted 23 June 2014

Available online 22 July 2014

Keywords:

Triazole
Schiff base complexes
Spectral
Thermal
Biological studies
DNA interaction

ABSTRACT

Manganese(II), cobalt(II), nickel(II) and copper(II) complexes of [(1H-1,2,4-triazole-3-ylimino)methyl]naphthalene-2-ol have been synthesized. The structure of complexes have been characterized by elemental analysis, molar conductance, magnetic moment measurements and spectral (IR, ¹H NMR, EI-mass, UV–Vis and ESR), and thermal studies. The results showed that the chloro and nitrate Cu(II) complexes have octahedral geometry while Ni(II), Co(II) and Mn(II) complexes in addition to acetato Cu(II) complex have tetrahedral geometry. The possible structures of the metal complexes have been computed using the molecular mechanic calculations using the hyper chem. 8.03 molecular modeling program to confirm the proposed structures. The kinetic and thermodynamic parameters of the thermal decomposition steps were calculated from the TG curves. The binding modes of the complexes with DNA have been investigated by UV–Vis absorption titration. The results showed that the mode of binding of the complexes to DNA is intercalative or non-intercalative binding modes. Schiff base and its metal complexes have been screened for their *in vitro* antimicrobial activities against Gram positive bacteria (*Staphylococcus aureus*), Gram negative bacteria (*Escherichia coli* and *Pseudomonas aeruginosa*), fungi (*Aspergillus flavus* and *Mucor*) and yeast (*Candida albicans* and *Malassezia furfur*).

© 2014 Elsevier B.V. All rights reserved.

* Corresponding author. Tel.: +20 40 3410037; fax: +20 40 3350804.

E-mail address: drnadia6@yahoo.com (N.A. El-Wakiel).

Introduction

DNA is an important drug target and it regulates many biochemical processes that occur in the cellular system. Many small molecules exert their anticancer activities by binding with DNA, thereby altering DNA replication and inhibiting the growth of tumor cells. Binding studies of small molecules to DNA are very important in the development of new therapeutic reagents and DNA molecular probes [1].

Transition metal complexes have been widely exploited for this purpose because by changing the ligand environment one can tune the DNA binding and cleaving ability of the metal complexes. The binding mechanisms between DNA and various redox substances, such as metal complexes [2–10], anticancer or antiviral drugs [11] and organic dyes [12] have been investigated. The importance criteria for the development of metallodrugs as chemotherapeutic agents are the ability of the metallodrug to bring about DNA cleavage. The DNA binding mechanism and behavior of the metal complexes are closely related to the size, shape and planarity of the intercalative ligands. It has been found that the coordination geometries and donor atoms of the ligands play key roles in determining the binding mode between metal complexes and DNA [13]. On the other hand, the metal ions and their flexible valences, which are responsible for the geometry of complexes, affect the intercalating ability of the metal complexes to DNA [14].

Schiff base complexes of transition metals are of particular interest to inorganic chemists because of their structural, spectral and chemical properties which are dependent on the nature of the ligand structure. Depending on their interesting structural properties and wide ranging uses, studies of Schiff base complexes have attracted the attention of many investigators. 1,2,4-Triazoles and their derivatives represent an interesting class of compounds possessing a wide spectrum of biological activities such as antifungal, anticancer, anti-inflammatory, antibacterial properties and antitumor [15–23] activities. Moreover, the metal complexes of 1,2,4-triazole derivatives have been extensively investigated [24–31].

Based on these facts and as part of our going studies on the synthesis, structural investigation and biological activity of Schiff bases metal complexes, we report here the synthesis and characterization of Mn(II), Co(II), Ni(II) and Cu(II) complexes of the titled Schiff base. All newly synthesized compounds have been characterized by microanalysis and spectroscopic methods (IR, ¹H NMR, EI-mass, UV–Vis and ESR), as well as thermal studies. The synthesized complexes were investigated for their DNA interaction using absorption titration. The Schiff base and its metal complexes have been screened for their *in vitro* antimicrobial activities against Gram positive bacteria (*Staphylococcus aureus*), Gram negative bacteria (*Escherichia coli* and *Pseudomonas aeruginosa*), fungi (*Aspergillus flavus* and *Mucor*) and yeast (*Candida albicans* and *Malassezia furfur*).

Experimental

Materials and methods

All compounds used in the present study were of pure grade available from BDH, Aldrich or Sigma. The solvents used for the spectral studies were spectroscopic grade from Aldrich.

The elemental microanalysis of the solid compounds were performed at the microanalytical center, Cairo University using Perkin–Elmer 2400 CHN Elemental analyzer. Metal content was estimated complexometrically using standard EDTA titration. Molar conductivities in DMF (10^{−3} M) at room temperature (25 °C) were measured using conductance bridge of the type 523

conductivity bridge. The Infrared spectra were recorded on a Perkin–Elmer 1430 IR spectrophotometer within the range 4000–200 cm^{−1} as KBr discs. Standard electron impact mass spectra (E.I.) were determined using a Finnigan MAT 8222 Spectrometer at 70 eV in micro analytical unit of Cairo University. The NMR spectra were carried out using a Varian Mercury-300BB NMR spectrophotometer operating at 300 MHz after dissolving the samples in d⁶-DMSO using tetramethylsilane as an internal standard. The electronic absorption spectra were recorded using a Shimadzu UV–Vis 240 spectrophotometer. The room temperature magnetic susceptibility of the solid samples was measured using magnetic susceptibility balance (Johnson Matthey) 436 Devon Park Drive employing the Gouy's method. The thermogravimetric analysis (TGA) of the solid samples were performed with the range 25–800 °C using the Shimadzu TG-50 thermogravimetric analyzer with different heating rate (5–20 °C/min.) under nitrogen atmosphere. The X-band electron spin resonance spectra of powder samples were recorded using Joel JES-FE2XG spectrometer model equipped with an E101 micro wave bridge at room temperature. The magnetic field was calibrated with diphenyl picryl hydrazyl (DPPH). The antimicrobial spectra of the prepared compounds were determined against the tested organisms on powdered samples using cut–plug method [32] in micro analytical unit, Botany Department, Faculty of Science, Tanta University.

Molecular modeling studies

An attempt to gain a better insight on the molecular structure of Metal complexes, geometric optimization and conformational analysis has been performed by the use of MM+ force field as implemented in hyperchem 8.0 [33]. Semi empirical method PM3 is then used for optimizing the full geometry of the system using Polak–Ribiere (conjugate gradient) algorithm and Unrestricted Hartree–Fock (UHF) is employed keeping RMS gradient of 0.01 kcal/mol. All the calculations refer to isolated molecules in vacuum.

DNA binding studies

The experiments were carried out in Tris–HCl buffer (5.0 mM of tris(hydroxymethyl)-aminomethane and 50 mM NaCl) at pH 7.2. Tris–HCl buffer was prepared using deionized and triple distilled water. Solutions of CT-DNA in Tris–HCl gave a ratio of UV absorbance at 260 and 280 nm (A₂₆₀/A₂₈₀) of 1.8–1.9, indicating that the DNA was sufficiently free from protein [34]. The stock solution of DNA was prepared by dissolving DNA in Tris–HCl buffer. Concentrated stock solutions of metal complexes were prepared by dissolving each complex in DMF and diluted suitably to the required concentration. Absorption titration experiments were performed with a fixed concentration of each complex (20 ppm), while gradually increasing the concentration of DNA. When the absorption spectra were measured, an equal amount of DNA was added to both the complex solutions and the reference solution to eliminate the absorbance of DNA itself.

For viscosity measurements, a viscometer was thermostated in water-bath maintained at 25 °C. The flow time for each sample was measured three times using digital stopwatch and an average flow time was calculated. The rate of flow of the DNA (3 × 10^{−5} M) and DNA with various concentrations of each complex were measured. The relative specific viscosity was calculated using the equation $\eta = (t - t_0)/t_0$, where t_0 is the flow time for the Tris–HCl buffer alone and t is the observed flow time for DNA in the absence and presence of the complex. Data are presented as $(\eta/\eta_0)^{1/3}$ vs. r (where $r = [\text{complex}]/[\text{DNA}]$), η_0 and η are the viscosity of DNA in the absence and presence of the complex [35,36].

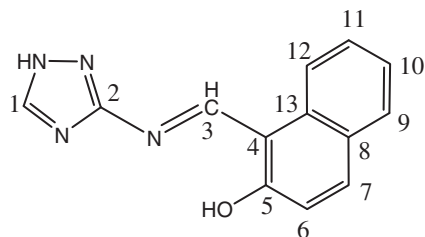


Fig. 1. Structure of the prepared Schiff base ligand (SB).

Antimicrobial activities

The antimicrobial spectrum of the prepared compounds was determined against the tested organisms on powdered samples using cut-plug method [37]. The prepared media heated in water bath with stirring, autoclaved, and poured in sterile petri dishes avoiding air bubbles, then left to solidify at room temperature. A regular well of 8 mm diameter on the center of each petri dish were cut using cork borer. plates were seeded with different micro-organisms and central wells were filled with 20 mg powder of the prepared ligands and some of their complexes for the tested bacteria, fungi and yeast, then incubated 24 h for bacteria and 48 h for fungi and yeast, after which the diameter of the inhibition zones were measured and the compounds which produced the highest inhibition zone was further assayed at different concentration in order to quantify its inhibitory effect using the turbidity method [38]. In this experiment, different concentrations of each complex was prepared in dimethylsulfoxide (DMSO) separately. The used concentrations were (30–1000 µg/ml), zero concentration was consider as a control. 0.5 ml of each standard organism suspension was mixed with 9.5 ml of each corresponding media in sterile test tube contained the tested complexes to give (30–1000 µg/ml). The results were recorded after incubation [39] in shaker incubator for 48 h. The turbidity of each mixture was measured then the turbidity of each mixture was measured and surviving ratio was calculated as a percentage of surviving cell number for each concentration to that of the original spore suspension at zero concentration (used as control) and finally the data are represented graphically.

Synthesis of Schiff-base ligand (SB)

The Schiff base ligand SB, (Fig. 1), was prepared by the condensation of 3-amino-1,2,4-triazole with 2-hydroxy-1-naphthaldehyde. A 1:1 mixture of them in hot methanol was refluxed for

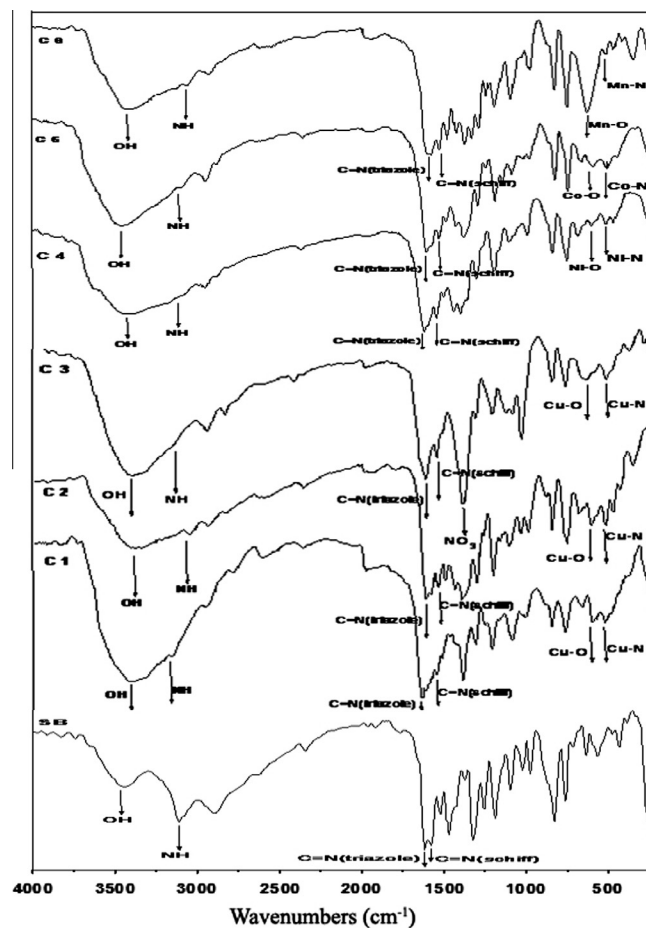


Fig. 2. Infrared spectra of ligand SB and its metal complexes.

8 h. This was achieved by refluxing 0.01 mol (1.72 g) of 2-hydroxy-1-naphthaldehyde with 0.01 mol (0.84 g) of 3-amino-1,2,4-triazole in methanol (100 ml) as a solvent. The condensation product separated on cooling was filtered off, washed several times with methanol till constant melting point and finally dried in a vacuum desiccator over anhydrous calcium chloride.

SB: ^1H NMR (300 MHz, DMSO- d_6) δ (ppm): 14.96 (s, 1H, NH), 10.79 (s, 1H, OH), 10.08 (s, 1H, CH=N), 8.42 (s, 1H, C1–H), 8.13 (d, J = 8.1 Hz, 1H, C12–H), 8.05 (d, 1H, J = 9 Hz, C7–H), 7.88 (d, 1H, J = 8.1 Hz, C9–H), 7.61 (dd, J = 8.1/7 Hz, C11–H), 7.43 (dd, 1H, J = 8.1/7 Hz, C10–H), 7.22 (d, 1H, J = 9 Hz, C6–H).

Table 1

Elemental analysis, molecular weight and physical properties of the prepared compounds.

Compounds	Molecular formula (empirical formula) (M.wt.)	m.p. (°C)	Elemental analysis				$A_m^{(b)}$
			%C ^(a)	%H ^(a)	%N ^(a)	%M ^(a)	
SB	C ₁₃ H ₁₀ N ₄ O (238.24)	240	65.54 (65.85)	4.2 (4.8)	23.52 (23.83)	–	–
1	[Cu ₂ L Cl ₃ (H ₂ O) ₅].H ₂ O (C ₁₃ H ₂₁ Cl ₃ Cu ₂ N ₄ O ₇) (578.78)	236	26.98 (27.29)	3.66 (3.28)	9.68 (9.95)	21.96 (21.38)	3.85
2	[Cu ₂ (L) ₂ (OAc)(MeOH)].OAc.H ₂ O (C ₃₁ H ₃₀ Cu ₂ N ₈ O ₈) (769.71)	>300	48.37 (47.48)	3.93 (3.71)	14.56 (14.81)	16.51 (16.17)	62.8
3	[Cu ₂ (L)(NO ₃) ₃ (H ₂ O) ₃ (MeOH) ₂].MeOH (C ₁₆ H ₂₇ Cu ₂ N ₇ O ₁₆) (700.51)	>300	27.43 (27.69)	3.88 (4.48)	14.00 (14.45)	18.14 (18.87)	17
4	[Ni ₃ (L) ₂ (OAc) ₄ (H ₂ O) ₂].MeOH (C ₃₅ H ₃₈ Ni ₃ N ₈ O ₁₃) (954.8)	>300	44.03 (43.84)	4.01 (3.99)	11.74 (11.91)	18.44 (18.44)	2.99
5	[Co ₃ (L) ₂ (OAc) ₄ (MeOH) ₂].H ₂ O.MeOH (C ₃₇ H ₄₄ Co ₃ N ₈ O ₁₄) (1001.59)	>300	44.37 (44.86)	4.43 (4.21)	11.19 (11.54)	17.65 (18.19)	4.54
6	[Mn ₂ (L) ₂ (OAc)(MeOH)].OAc.H ₂ O (C ₃₁ H ₃₀ Mn ₂ N ₈ O ₈) (752.49)	>300	49.48 (49.71)	4.02 (3.91)	14.89 (15.21)	14.60 (15.12)	69.46

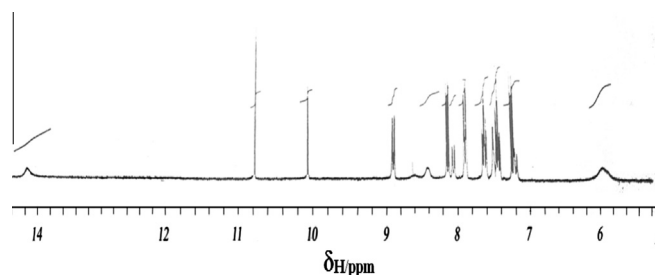


Fig. 3. ^1H NMR spectra of ligand SB.

Synthesis of complexes

All the complexes were prepared by refluxing 1 mmol of the Schiff base ligand dissolved in methanol with 1 mmol of each metal salt dissolved in methanol, where either copper salts (acetate, chloride, or nitrate), manganese acetate, cobalt acetate, or nickel acetate was used as a metal source. The mixtures were then refluxed under stirring for 4 h. The solid complexes which separated out on hot were filtered off, washed several times with methanol and finally dried in a vacuum desiccator over anhydrous CaCl_2 .

Results and discussion

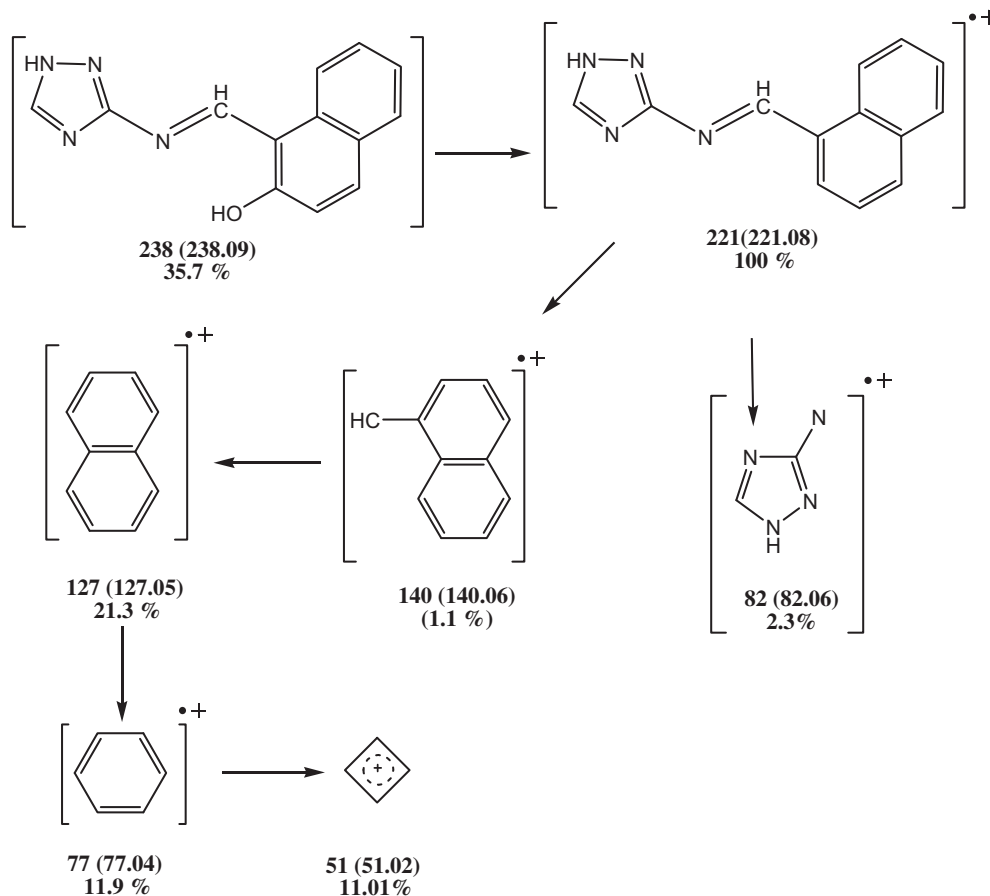
The elemental analysis and molar conductance results

The stoichiometry and formulation of the metal complexes are based on their elemental analyses, molar conductivity and IR spectral data. The results of elemental analysis and molar conductance

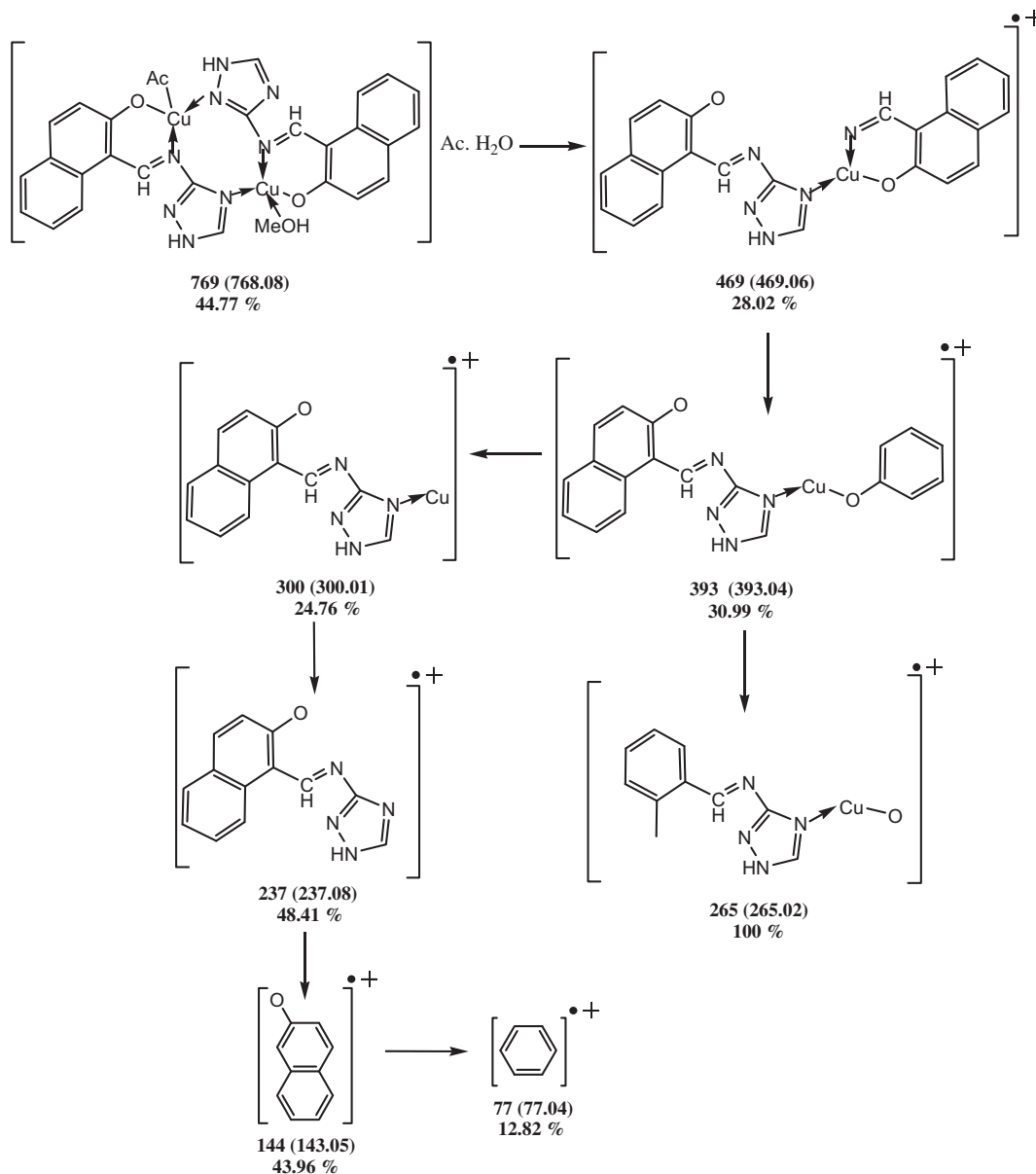
are collected in Table 1. The results of elemental analysis obtained are in good agreement with those calculated for the suggested molecular formulas. The low molar conductance values of complexes 1, 3, 4 and 5 revealed that these complexes are non-electrolytes in DMF [40]. Complexes 2 and 6 have molar conductance values of 62.8 and $69.4 \text{ ohm}^{-1} \text{ mol}^{-1} \text{ cm}^2$, respectively, in DMF, which is in accordance with 1:1 electrolytes. The electrolytic nature of these complexes was further confirmed by the addition of FeCl_3 solution to the DMF solution of these complexes which result in the formation of red brown coloration confirming the non coordination of one acetate ion.

Infrared absorption spectra

The infrared spectra exhibited by the Schiff-base ligand (SB) and its complexes are given in Fig. 2 whereas the important IR spectral bands and their assignments are given in Table S1. The IR spectra of the free ligand showed two bands at 3426 cm^{-1} and 3102 cm^{-1} which assigned to phenolic OH and NH groups, respectively. The strong and intense bands appearing at 1613 cm^{-1} and 1572 cm^{-1} are due to $\nu_{\text{C=N}}$ of triazole moiety and azomethine group, respectively. These bands were shifted to higher or lower frequencies on complex formation. This shift is due to coordination of triazole and azomethine nitrogen to the metal center. IR spectra of all complexes showed broad bands at $3370\text{--}3425 \text{ cm}^{-1}$ which can be assigned to ν_{OH} of water or methanol molecules solvates. The presence of coordinated or lattice water or methanol molecules renders it difficult to follow the behavior of the OH groups in complex formation from the stretching vibration region. The complexes 2, 4, 5 and 6 have two bands at $1581\text{--}1593 \text{ cm}^{-1}$ and $1386\text{--}1393 \text{ cm}^{-1}$ assigned to ν_{asy} and ν_{sym} of the acetate ion, respectively. The



Scheme 1. The proposed fragments of Schiff base ligand (SB).



Scheme 2. The proposed fragments of Cu complex 2.

Table 2
ESR spectral data of Cu(II) complexes.

Complex	$g_{ }$	g_{\perp}	g_{eff}	$A_{ }$	$g_{ }/A_{ }$	G
1	2.257	2.076	2.156	94.28	–	3.35
2	2.281	2.093	2.136	92.86×10^{-4}	245.26	3.021
3	2.231	2.06	2.085	128.57	–	3.85

difference between those two bands is $192\text{--}200\text{ cm}^{-1}$ which suggests that the acetate group is monodentate [41].

The IR spectrum of complex 3 showed a strong band at 1382 cm^{-1} which assigned to monodentate nitrate coordination. For complex 1, a weak band appeared at 279 cm^{-1} due to M–Cl mode. The participation of oxygen and nitrogen atoms in coordination to the metal ion is further supported by the appearance of non-ligand bands within the range $572\text{--}628$ and $499\text{--}514\text{ cm}^{-1}$ due to $\nu_{\text{M-O}}$ and $\nu_{\text{M-N}}$ respectively.

¹H NMR spectra

The ¹H NMR spectrum of the Schiff base ligand (SB) is shown in Fig. 3 in which signals corresponding to the aromatic hydrogen appeared within the range 7.22–8.13 ppm. The spectrum of the ligand showed a singlet at 10.08, 10.79 and 14.96 ppm corresponding to CH=N, OH and NH protons, respectively. The heteroaromatic proton appeared as a singlet at 8.42 ppm.

El-mass spectra

The El-mass spectrum of Schiff base ligand (SB) showed a molecular ion peak at m/z 238 that is equivalent to its molecular weight [L]⁺. The peaks due to the various fragments appeared at m/z 221(100% base peak), 169 (39.9%), 139 (1.1%), 127 (21.3%), 77 (11.9%), 63 (22.5%), 51 (11.1%) which correspond to the fragments shown in Scheme 1.

The molecular ion peaks of complexes have been used to confirm the proposed formula. The multiplex patterns of the mass spectra give an impression of the successive degradation of the compounds with the series of peaks corresponding to the various fragments. All these fragments led to the formation of the species $[ML]^+$ which underwent demetallation to form the species $[L]^+$. The proposed fragmentation pattern of complex 2, as a representative example, is shown in Scheme 2. The first peak appearing at m/z 769 (44.77%) represents the molecular ion peak of the complex. For other metal complexes, the peaks observed at m/z 578, 700, 954, 998 and 754 for complexes 1, 3, 4, 5 and 6, respectively, correspond to the molecular ion peaks of these compounds. The results of both elemental analyses and mass spectra of the prepared complexes are in satisfactory agreement with each other, which confirmed the proposed molecular formulas.

Magnetic susceptibility studies

The subnormal μ_{eff} values of Cu(II) complexes (1.42, 1.44 and 1.4 B.M. for complexes 1, 2 and 3, respectively) reveals the Cu–Cu interaction. The magnetic moment value of Ni(II) complex 4 (3.26 B.M) lies in the range reported for a tetrahedral structure. The observed magnetic moment of Co(II) complex 5 was found to be 4.18 B.M [42] indicating the presence of three unpaired electrons in the d-orbital in tetrahedral structure. Mn(II) complex 6 has low magnetic moment (5.27 B.M) due to metal–metal interaction.

The electronic absorption spectra

The Nujoll mull electronic spectra of the Cu(II) complexes 1 and 3 displayed two bands at 14,793 and 24,390 cm^{-1} for complex 1 and at 14,706 and 23,809 cm^{-1} for complex 3 which can be assigned to ${}^2B_{1g} \rightarrow {}^2B_{2g}$ and ${}^2B_{1g} \rightarrow {}^2E_g$ transition, respectively indicating distorted octahedral geometry around the metal center. The Cu(II) complex 2 displayed two absorption bands at 14,925 and 23,256 cm^{-1} which are attributed to ${}^2T_2 \rightarrow {}^2E_2$ and charge transfer transitions, respectively, in tetrahedral Cu(II) complexes [43]. The spectrum of Ni(II) complex 4 showed a medium intensity band at 16,949 cm^{-1} assignable to ${}^3T_1 \rightarrow {}^3T_1(P)$ v_3 transition in a tetrahedral structure. The electronic spectrum of Co(II) complex 5 exhibited a band at 14,925 cm^{-1} which is assigned to

${}^4A_2 \rightarrow {}^4T_1(P)$ transition due to tetrahedral arrangement. The Mn(II) complex 6 showed, two broad bands at 15,151 and 22,727 cm^{-1} corresponding to ${}^6A_1 \rightarrow {}^4T_2(G)$ and ${}^6A_1 \rightarrow {}^4E(G)$ transition, respectively, which corresponds to a tetrahedral structure.

Electron Spin Resonance (ESR)

The X-band ESR spectra of Cu(II) complexes have been recorded in the solid state at room temperature and the ESR spectral parameters (g_{eff} , g_{\parallel} , g_{\perp}) are calculated and listed in Table 2. As set of g values satisfying $g_{\parallel} > g_{\perp}$ indicates the unpaired electron most likely resides in the $d_{x^2-y^2}$ (or less likely d_{xy}) ground state orbital [44]. The g_{\parallel} is moderately sensitive function for indicating covalency of the metal–ligand bonding, in which g_{\parallel} is normally 2.3 or larger for ionic bonding and less than this value for covalent bonding [45]. The g_{\parallel} values of complexes 1, 2 and 3 are less than 2.3 indicative of a significant degree of covalent bonding. The positive contribution in g_{eff} values of the complexes under investigation (1, 2 and 3) than the value of free electron (2.0023) indicated an increase in the covalent nature of bonding between the metal ion and ligand molecules. The $g_{\parallel}/A_{\parallel}$ may be considered as an empirical index of tetrahedral distortion and square planar geometry [46]. The range reported for square planar complexes is 105–135 cm^{-1} and for tetrahedral distorted complexes 150–250 cm^{-1} . The $g_{\parallel}/A_{\parallel}$ value of complex 2 is 245.26 cm which lies in the range expected for tetrahedral rather than square planar complexes. The g values are related to the axial symmetry parameter, G , by the expression $G = (g_{\parallel} - 2)/(g_{\perp} - 2)$, which indicates the extent of exchange interaction between copper centers in polycrystalline solids. If the G value is greater than four, the exchange interaction is negligible, while a value less than four indicates a considerable exchange interaction in the complex [47]. The G value of complexes 1, 2 and 3 were found to be less than four (3.021, 3.38 and 3.85, respectively) suggesting considerable interactions in the solid state.

Thermogravimetric analysis of the complexes

The thermal behavior of the metal complexes was studied using TG technique. The stages of decomposition, temperature range, weight loss percentages as well as decomposition products are given in Table 3. The thermal decomposition of complex 1, as an example, takes place in three steps. The first decomposition step

Table 3
Thermogravimetric analysis data (TGA) of the metal complexes.

No	Molecular formula	Temp. range (°C)	Mass loss%		Assignment
			Found	Calc.	
1	$[\text{Cu}_2\text{L Cl}_3(\text{H}_2\text{O})_5] \cdot \text{H}_2\text{O}$	26–93	3.03	3.11	Loss of hydrated H_2O molecule
		93–295	14.79	15.59	Loss of 5 coordinated H_2O
		295–580	54.62	53.72	Loss of Cl^- anions and decomposition of the organic ligand with formation of CuO
2	$[\text{Cu}_2(\text{L})_2(\text{OAc})(\text{MeOH})] \cdot \text{OAc} \cdot \text{H}_2\text{O}$	32–109	2.82	2.34	Loss of 1 hydrated H_2O molecule
		109–442	19.75	19.5	Loss of 1 MeOH molecule, and the two acetate anions
		442–604	25	24.71	Dissociation of two triazole rings and 2(CH = N)
		604–718	33.06	32.76	Further decomposition of the organic ligand with formation of CuO as final product
3	$[\text{Cu}_2\text{L}(\text{NO}_3)_3(\text{H}_2\text{O})_3(\text{MeOH})_2] \cdot \text{MeOH}$	40–100	3.97	4.5	Loss of 1 MeOH molecule
		100–252	16.79	16.85	Loss of 3 H_2O and 2 MeOH
		252–630	54.94	55.85	Decomposition of the organic ligand with formation of CuO as final product
4	$[\text{Ni}_3(\text{L})_2(\text{OAc})_4(\text{H}_2\text{O})_2] \cdot \text{MeOH}$	42–100	3.35	3.63	Loss of 1 MeOH molecule
		100–643	67.42	68.29	Loss of 2 coordinated H_2O , acetate anions and dissociation of the organic ligand forming NiO_2 as final product
5	$[\text{Co}_2(\text{L})_2(\text{OAc})_4(\text{MeOH})_2] \cdot \text{H}_2\text{O} \cdot \text{MeOH}$	30–100	5.33	4.99	Loss of 1 H_2O and 1 MeOH
		100–470	71.43	72.49	Loss of 2 MeOH molecule, acetate anions and dissociation of the organic ligand with formation of CoO as final product
6	$[\text{Mn}_2(\text{L})_2(\text{OAc})(\text{MeOH})] \cdot \text{OAc} \cdot \text{H}_2\text{O}$	33–111	2.54	2.39	Loss of 1 hydrated H_2O molecule
		111–359	11.63	12.1	Loss of 1 MeOH and outer acetate molecule
		359–882	65.45	66.6	Loss of coordinated acetate anion and dissociation of the organic ligand forming MnO as final product

appeared within the temperature range 26–93 °C with mass loss of 3.03% which corresponded to elimination of one hydrated water molecule. The second step appeared at 93–295 °C with mass loss of 14.79%, assigned to the elimination of five coordinated water molecules. The third step above 295 °C represents the volatilization of Cl⁻ anions and degradation of the organic ligand leaving CuO as the final product.

Mechanistic and non-mechanistic methods were used to determine the kinetic data from TG curves. The kinetic parameters of activation energy (*E*), reaction order (*n*) and frequency factor (*A*) were obtained from TG data by non-isothermal integral method proposed by Coats–Redfern [48] and by approximation method proposed by Horowitz–Metzger [49]. The values obtained by approximation method were different from those calculated by integral method due to the different mathematical treatment of the obtained data [50]. The kinetic parameters obtained from the previously mentioned methods are listed in Tables S1 and S2.

The thermodynamic activation parameters namely, enthalpy (ΔH^*), entropy (ΔS^*) and free energy of decomposition (ΔG^*) were evaluated using the following relationships:

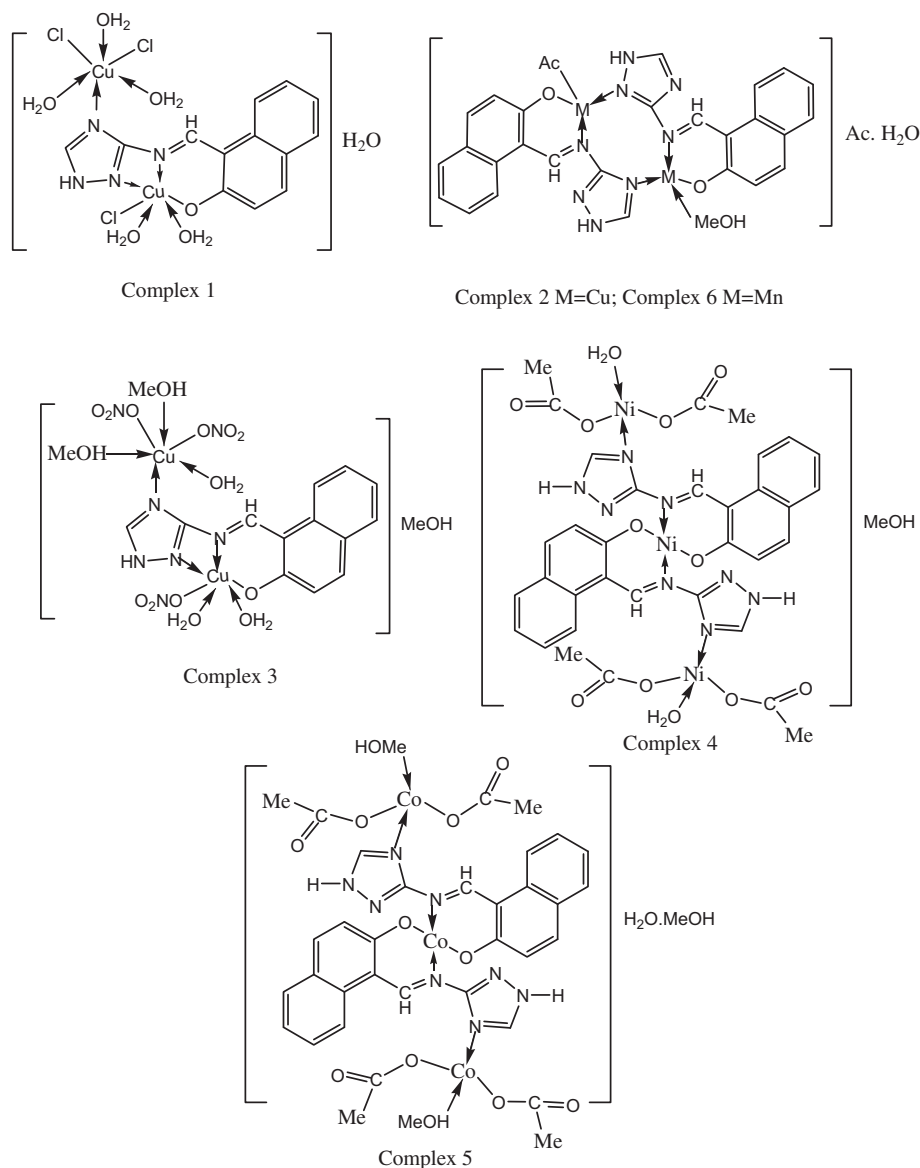
$$\Delta H^* = E^* - RT$$

$$\Delta S^* = R[\ln(Ah/kT) - 1]$$

$$\Delta G^* = \Delta H^* - T\Delta S^*$$

where *k* is Boltzmann constant and *h* is Planck's constant. From the above results, the following features can be deduced:

1. The negative values of the activation entropies ΔS^* indicate a more ordered activated complex than the reactants and/or the reactions are slower than normal.
2. The positive values of the ΔH^* mean that the decomposition processes are endothermic.
3. Kinetics of the thermal decomposition stages of all complexes under study obeys, in most cases, the first order kinetics.
4. The values of activation energies increase as the maximum temperature of decomposition increases reflecting higher stability of the complexes formed under investigation.
5. The positive values of ΔG^* suggested that this is a non-spontaneous process.
6. It was found that the order of the activation energy values of the first decomposition step for the acetato complexes is complex 5 > complex 4 > complex 6 > complex 2 while for Cu(II) complexes of different anion the order is complex 3 > complex



Scheme 3. Structures of the prepared complexes.

1 > complex 2. This differences may be due to the structure of the complexes and the electronic configuration of the metal(II) ion.

Molecular modeling studies

Since single crystals could not be grown for the complexes under investigation, it was thought worthwhile to obtain structural information through molecular modeling. Based on the stereochemistry of the metal complexes proposed on the basis of analytical and spectroscopic studies, the possible structures of some selected metal complexes have been computed using the molecular mechanic calculations by the hyper chem. 8.03 molecular modeling program. The molecular modeling of the free ligand and its complexes (Figs. S1–S7) showed the following:

- (i) A large variation in C=N bond length on coordination via the N-atom of group azomethine.
- (ii) The absence of O—H as well as the appearance of M—O bond indicated the participation of phenolic O—H in complex formation [51].
- (iii) The bond angles of Schiff base moiety are altered somewhat upon coordination.

Selected calculated bond lengths and angles of metal complexes are presented in Table S4.

Based on the information gained from the previous studies, the structure of complexes formed between the ligand with the metal ion [Mn(II), Co(II), Ni(II) and Cu(II)] can be represented in Scheme 3.

DNA binding interaction

Electronic absorption titration

The DNA binding studies of metal complexes with CT DNA were carried out by employing electronic absorption spectral titration. It is a general observation that hypochromicity in the absorption spectra accompanies the binding of the molecules to DNA [52]. The absorption titration was performed by keeping the concentration of the complex constant while varying the DNA concentration. The extent of the spectral change is related to the strength of binding.

Figs. 4 and 5 show the absorption spectra of complexes 2 and 4 at constant complex concentration in the absence and presence of calf-thymus (CT) DNA.

The electronic absorption spectra of complexes 2 and 4 consist of two bands. The absorption band centered at 425 nm is assigned to metal-to-ligand charge transfer (MLCT) transition. The second band at 329 and 320 nm for complexes 2 and 4, respectively, is attributed to $\pi-\pi^*$ transition. With increasing concentration of CT-DNA, the electronic spectra of complexes 2 and 4 showed a clear hypochromism of about 10.27% and 13.4% and bathochromism of 4 nm and 3 nm for complexes 2 and 4, respectively. These spectral characteristics suggested that both complexes interact with CT DNA by the intercalative binding modes, because intercalation, in most cases, leads to hypochromism and bathochromism in the electronic absorption spectra [53].

The intercalative mode involve a stacking interaction between an aromatic chromophore and the base pairs of DNA [54] while hypochromism is a spectral feature depicting non-covalent interactions, particularly electrostatic, groove binding resulting from the damage of secondary structure of the DNA double helix. The extent of the hypochromism is commonly consisting with the strength of intercalative interaction [55].

On the other hand, the absorption spectra of complexes 1 and 6 presented hyperchromism upon titration with DNA. As the DNA

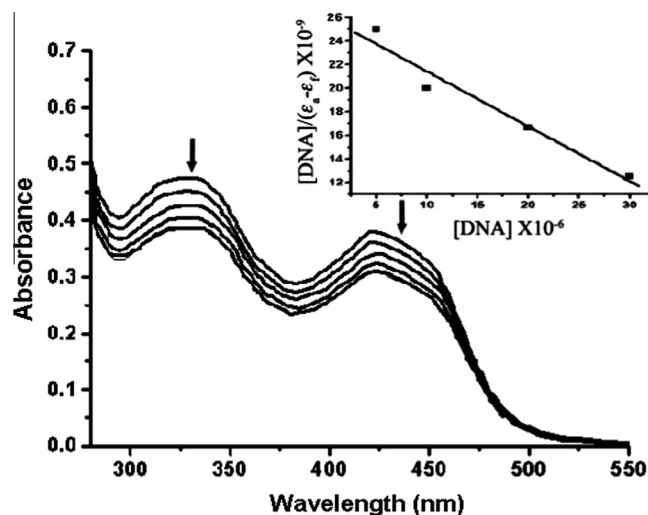


Fig. 4. (left) Absorption spectra of complex 2 upon the titration with CT-DNA. Arrows indicates the change upon increasing the concentration of CT-DNA from 0 to 40 μM . [Complex] = 25 μM , (right) plot of $[\text{DNA}]/(\epsilon_a - \epsilon_f)$ vs. $[\text{DNA}]$ for the absorption titration of CT-DNA with the complex.

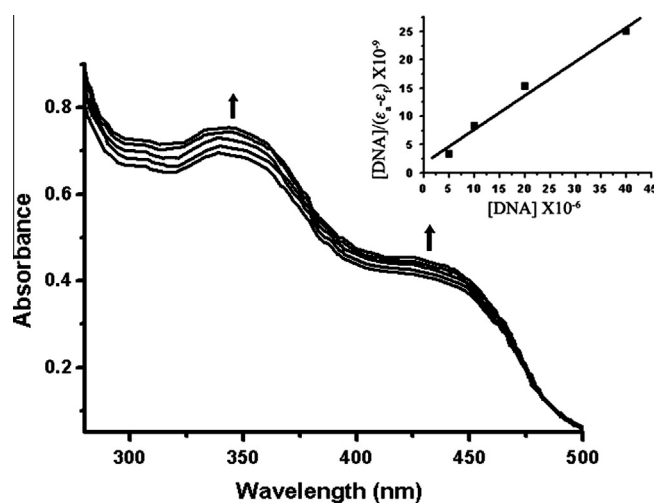


Fig. 5. (left) Absorption spectra of complex 6 upon the titration with CT-DNA. Arrow indicates the change upon increasing the concentration of CT-DNA from 0 to 40 μM . [Complex] = 25 μM , (right) Plot of $[\text{DNA}]/(\epsilon_a - \epsilon_f)$ vs. $[\text{DNA}]$ for the absorption titration of CT-DNA with the complex.

concentration is increased, the $\pi-\pi^*$ transition bands appearing at 318 and 340 nm, for complexes 1 and 6, respectively, yielding an absorbance hyperchromism of 4.46% and 41.34% for complexes 1 and 6, respectively, without change in wavelength. This implies that some interaction occurred between complex and the surface of DNA molecule and the interaction is not an intercalation [56]. The strong hyperchromism of complex 6 suggests a mode of binding that involves a stacking interaction between the complex and the base pairs of DNA [57].

To quantify the extent of binding of the complexes with CT-DNA, the intrinsic binding constant K_b was calculated by monitoring the change in the absorbance of the metal to ligand transfer band (MLCT), with increasing the concentration of DNA using the following equation:

$$[\text{DNA}]/(\epsilon_a - \epsilon_f) = [\text{DNA}]/(\epsilon_b - \epsilon_f) + 1/K_b(\epsilon_b - \epsilon_f)$$

where $[\text{DNA}]$ is the concentration of DNA in base pairs, the apparent absorption coefficients ϵ_a , ϵ_f and ϵ_b correspond to $A_{\text{obsd}}/[\text{Metal}]$, the

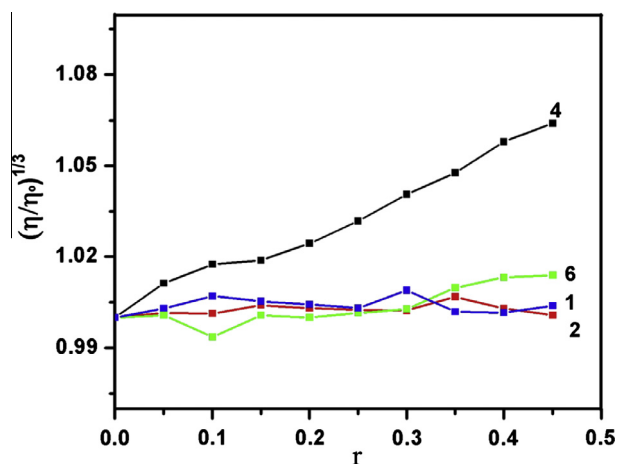


Fig. 6. Effect of the increasing amount of complexes 1, 2, 4 and 6 on the relative viscosity of CT-DNA at 25 °C, [DNA] is 3×10^{-5} M.

extinction coefficient for the free complex and the extinction coefficient for the bound complex, respectively. In plots of $[\text{DNA}]/(\varepsilon_a - \varepsilon_f)$ vs. $[\text{DNA}]$, K_b is given by the ratio of the slope to the intercept through a plot of $[\text{DNA}]/(\varepsilon_a - \varepsilon_f)$ vs. $[\text{DNA}]/(\varepsilon_b - \varepsilon_f)$.

For complex 6, the K_b value $3.45 \times 10^5 \text{ M}^{-1}$ suggests a strong binding of Mn-complex 6 with DNA close enough to the classical intercalator Ethidium bromide binding affinity to DNA ($K_b = 1.23 \times 10^5 \text{ M}^{-1}$) [57].

For Cu(II) complexes 1 and 2, the higher K_b value obtained for complex 1 suggests that more base pairs are available for binding than in complex 2. The lower K_b value of complex 2 indicates the non-intercalative binding interaction with DNA and probable groove binding or external binding is suggested [56].

Also, the K_b values for Cu-complexes are of:

- (i) Lower magnitude than that of the Cu complexes reported in the literature such as DNA intercalator $[\text{Cu}(\text{TAN})(\text{O}_2\text{CMe})]$, ($K_b = 9.8 \times 10^5 \text{ M}^{-1}$ [58]; $[\text{Cu}(\text{flmq})_2(\text{py})_2]$, ($K_b = 8.12 \times 10^5 \text{ M}^{-1}$) [59] and $[\text{Cu}(\text{dthp})\text{Cl}_2]$ ($K_b = 6.9 \times 10^5 \text{ M}^{-1}$) [60].
- (ii) Larger than that of $[\text{Cu}(\text{Itpy})_2](\text{ClO}_4)$ ($K_b = 4.26 \times 10^3 \text{ M}^{-1}$) [61]; $[\text{Cu}(\text{bpy})(\text{Gly})\text{Cl}]\cdot 2\text{H}_2\text{O}$, ($K_b = 1.84 \times 10^3 \text{ M}^{-1}$) [10].
- (iii) COMPARABLE to $[(\text{phen})\text{Cu}(\mu\text{-bipp})\text{Cu}(\text{phen})]\text{ClO}_4$ ($K_b = 1.6 \times 10^4 \text{ M}^{-1}$ [62]) $[\text{Cu}(\text{imda})(\text{dpq})]$, ($K_b = 1.7 \times 10^4 \text{ M}^{-1}$ [63].

Viscosity measurements

The optical methods cannot be used exclusively to prove intercalation so other methods such as viscosity measurement is

needed to be taken together to determine the DNA binding mode of complexes. The viscosity studies provide a strong argument for intercalation. The viscosity measurement is based on the flow rate of a DNA solution through a capillary viscometer. A classical interaction mode results in lengthening the DNA helix as base pairs are separated to accommodate the binding ligand leading to the increase of DNA viscosity. On the other hand, a complex that binds exclusively in the DNA grooves by partial and/or non-classical intercalation typically causes less pronounced (positive or negative) or no change of viscosity in DNA solution.

The effect of increasing amount of complexes on the relative viscosity of DNA is shown in Fig. 6. The data obtained reveals that:

- (i) For complex 4, the relative viscosity of DNA is increased by increasing the concentration of complex 4. This phenomenon may be explained by the insertion of the compound in between the DNA base pairs, leading to an increase in the separation of base pairs at intercalation sites and an increase in overall DNA length. The increase in DNA viscosity in case of complex 4 suggests that complex 4 combined to DNA via intercalative binding mode.
- (ii) The viscosity of DNA remains almost unchanged upon addition of complexes 1, 2 and 6 suggesting non-intercalative and probably groove binding mode of complexes [64].

Antimicrobial activity

The biological activity of the synthesized Schiff base ligand (SB) and its metal complexes have been studied for their antimicrobial activity against Gram positive bacteria (*S. aureus*), Gram negative bacteria (*E. coli* and *P. aeruginosa*), fungi (*A. flavus* and *Mucor*) and yeast (*C. albicans* and *M. furfur*). These organisms were chosen as they are known as human pathogens. Tetracycline, Amphotericin B and Streptomycin were used as standard drugs. The capability of the prepared compounds to inhibit the growth of microorganisms was tested on solid media through of inhibition zone diameter; the obtained data are shown in Table 4. It was observed that SB is active against Gram negative bacteria (*E. coli*), Gram positive bacteria, fungi (*A. flavus*) and yeast (*M. furfur*) (diameters inhibition zone ranged between 16 and 30 mm). The Cu(II) complex 1 showed activity against all the tested organisms (diameters inhibition zone ranged between 14 and 30 mm) except the yeast, *M. furfur*. The results showed also that complex 3 showed activity against fungi, one type of Gram negative bacteria (*E. coli*) and yeast (*C. albicans*). The Ni(II) complex 4 showed the highest activity against *A. flavus* with inhibition zone diameters 45 mm. It also showed activity against *E. coli* and *A. flavus*. The Co(II) complex 5 was active against Gram negative, fungi and *C. albicans*, and gave the highest activity

Table 4

Inhibition zone diameter (mm) produced by 0.02 g ligands and its complexes against different organisms.

Compounds	Organisms						
	Bacteria			Fungi		Yeast	
	<i>E. coli</i>	<i>P. aureus</i>	<i>St. aureus</i>	<i>A. flavus</i>	<i>Mucor</i>	<i>M. furfur</i>	<i>C. albicans</i>
SB	16	–ve ^a	20	21	–ve	30	–ve
1	25	14	19.5	20	28	–ve	32
3	20	–ve	–ve	18.5	13	–ve	10
4	19	–ve	–ve	45	–ve	–ve	–ve
5	28	11	–ve	45	10	–ve	25
Tetracycline ^b	33	30	30	–	–	–	–
Amphotericin B ^c	–	–	–	20	18	–	20
Streptomycin ^d	–	–	–	–	–	17	–

^a Inactive against the tested organism.

^{b,c,d} Standard drugs used.

Table 5

The ratio of surviving cell number of *A. flavus* in the presence of different concentrations of complexes 4 and 5 using turbidity method.

Comp	Conc.($\mu\text{g/ml}$)						
	0	30	60	120	250	500	1000
	% Surviving ratio						
4	100	90	75	54	33.5	20	5
5	100	46.5	20	15.65	10	9.5	7.5

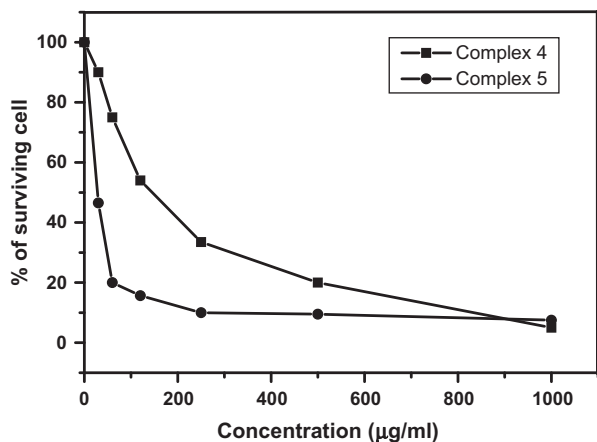


Fig. 7. The ratio of surviving cell number of complexes 4 and 5 with *A. flavus*.

against *A. flavus*. The obtained data indicated that the resulting metal complexes enhanced, in most cases, the bio-activity of the free ligand.

Since compounds 4 and 5 exhibited relatively high activity against *A. flavus*, different concentrations of them in dimethylsulfoxide were tested for their surviving ratio against *A. flavus* using turbidity method [65]. The ratio of the turbidity for the media containing the complex to those without the complex is taken as indicator for the surviving cell number. Table 5 and Fig. 7 illustrated that complex 5 is more potent than complex 4. The obtained data indicated also that a concentration of 170 and 32 g/ml of complexes 4 and 5, respectively, were enough to kill 50% of the tested microorganism which are relatively low concentrations, especially for complex 5.

Conclusion

In the present study, five new metal complexes of Schiff base derived from 1,2,4-triazole and 2-hydroxy-1-naphthaldehyde were synthesized and characterized by elemental, mass spectra, thermal analyses, IR, spectral, and magnetic data. The spectral data suggested distorted octahedral and tetrahedral geometry for Cu(II) complexes and tetrahedral geometries for Ni(II), Co(II) and Mn(II) complexes which are consistent with the geometry optimization and conformational analysis. The values of E , A , (ΔH^*), (ΔS^*) and (ΔG^*) as well as the most probable mechanism were reported.

The interaction of the metal complexes 1, 2, 4 and 6 with CT-DNA has been investigated by using absorption spectra and viscosimetry measurements. The obtained results indicate that the interaction mode between complex 4 and DNA is intercalative binding mode while complexes 1, 2 and 6 interact with DNA via non-intercalative and probably groove binding mode of binding. The ligand (SB) and its complexes were also tested for their antimicrobial activities. The obtained data indicated that the resulting

metal complexes enhanced, in most cases, the antimicrobial activity of the free ligand.

Acknowledgment

The authors are thankful to Prof. Dr. Y.A.G. Mahmoud, Tanta University, Faculty of Science, Botany Department, for his assistance to obtain the biological results of the synthesized compounds.

Appendix A. Supplementary material

Supplementary data associated with this article can be found, in the online version, at <http://dx.doi.org/10.1016/j.molstruc.2014.06.071>.

References

- [1] Y. Liu, H. Chao, Y. Yuan, H. Yu, L. Ji, *Inorg. Chim. Acta* 359 (2006) 3807–3814.
- [2] B. Lippert, *Prog. Inorg. Chem.* 54 (2005) 385–447.
- [3] E. Efthimiadou, N. Katsaros, A. Karaliota, G. Psomas, *Inorg. Chim. Acta* 360 (2007) 4093–4102.
- [4] Y. Liu, X. Guan, X. Wei, L. He, W. Mei, J. Yao, *Transition Met. Chem.* 33 (2008) 289–294.
- [5] A. Kulkarni, S. Patil, P. Badami, *Eur. J. Med. Chem.* 44 (2009) 2904–2912.
- [6] G. Sathyaraj, T. Weyhermuller, B. Nair, *Eur. J. Med. Chem.* 45 (2010) 284–291.
- [7] Z. Yan, Z. Xu, G. Dai, H. Liang, S. Zhao, *J. Coord. Chem.* 63 (2010) 1097–1106.
- [8] J. Qian, X. Ma, H. Xu, Y. Tian, J. Shang, Y. Zhang, S. Yan, *Eur. J. Inorg. Chem.* (2010) 3109–3116.
- [9] M. Patel, D. Gandhi, P. Parmar, *Spectrochim. Acta, A* 84 (2011) 243–248.
- [10] M. Mohamed, A. Shoukry, A. Ali, *Spectrochim. Acta, A* 86 (2012) 562–570.
- [11] Z. Zhu, C. Li, N. Li, *Microchem. J.* 71 (2002) 57–63.
- [12] I. Ho, G. Lee, W. Chung, *J. Org. Chem.* 72 (2007) 2434–2442.
- [13] V. Manikandamathavan, V. Rajapandian, A. Freddy, T. Weyhermuller, V. Subramanian, B. Nair, *Eur. J. Med. Chem.* 57 (2012) 449–458.
- [14] P. Vigato, S. Tamburini, L. Bertolo, *Coord. Chem. Rev.* 251 (2007) 1311–1492.
- [15] L. Labanauskas, E. Udrenaite, P. Gaidelis, A. Brukstus, *Il Farmaco* 59 (2004) 255–259.
- [16] G. Turan-Zitouni, Z.A. Kaplanckh, M.T. Yildiz, P. Chevallet, D. Kaya, *Eur. J. Med. Chem.* 40 (2005) 607–613.
- [17] K. Singh, M.S. Barwa, P. Tyagi, *Eur. J. Med. Chem.* 41 (2006) 147–153.
- [18] B. Tozkoparan, E. Kupeli, E. Yesilada, M. Ertan, *Bioorg. Med. Chem.* 15 (2007) 1808–1814.
- [19] G.B. Bagihalli, P.G. Avaji, S.A. Patil, P.S. Badami, *Eur. J. Med. Chem.* 43 (2008) 2639–2649.
- [20] Z.A. Kapalcikli, G.T. Zitoungi, A. Ozdemir, G. Reval, *Eur. J. Med. Chem.* 43 (2008) 155–159.
- [21] H. Kumar, S. Javed, S. Khan, M. Amir, *Eur. J. Med. Chem.* 43 (2008) 2688–2698.
- [22] K.S. Bhat, B. Poojary, D.J. Prasad, P. Naik, B.S. Holla, *Eur. J. Med. Chem.* 44 (2009) 5066–5070.
- [23] N. Guzeldemirci, O. Kucukbasmac, *Eur. J. Med. Chem.* 45 (2010) 63–68.
- [24] P. Banerjee, O.P. Pandey, S.K. Sengupta, *Transition Met. Chem.* 33 (2008) 1047–1052.
- [25] M. Ghassemzadeh, L. Fallahnedjad, M.M. Heravi, B. Neumüller, *Polyhedron* 27 (2008) 1655–1664.
- [26] S. Şenery, A. Erçağ, O.S. Şentürk, E. Perpelek, F.U. Sinan, *J. Coord. Chem.* 61 (2008) 740–749.
- [27] O. Bekircan, Z. Bıyıklıoğlu, I. Acar, H. Bektas, H. Kantekin, *J. Organomet. Chem.* 693 (2008) 3425–3429.
- [28] Z. Li, Z. Gu, K. Yin, R. Zhang, Q. Deng, J. Xiang, *Eur. J. Med. Chem.* 44 (2009) 4716–4720.
- [29] A.M. Khedr, M. Gaber, E.H. Abd El-Zaher, *Chin. J. Chem.* 29 (2011) 1124–1132.
- [30] A. Singh, O. Pandey, S. Sengupta, *Spectrochim. Acta, A* 85 (2012) 1–6.
- [31] R.M. Issa, M. Gaber, N.A. Al-Wakiel, S.K. Fathalla, *Chin. J. Chem.* 30 (2012) 547–556.
- [32] T. Pridham, L. Lindenfelser, O. Shotwell, F. Stodola, R. Bendict, C. Foley, P. Jacks, W. Zaumeyer, W. Perston, J. Mitchell, *Phytopathology* 46 (1956) 568.
- [33] HyperChem, Release 8.03 for Windows, Molecular modeling system, Hypercube Inc., 2007.
- [34] J. Marmur, *J. Mol. Biol.* 3 (1961) 208–218.
- [35] J.B. Chaires, N. Dattagupta, D.M. Crothers, *Biochemistry* 21 (1982) 3933.
- [36] G. Cohen, H. Eisenberg, *Biopolymers* 8 (1969) 45.
- [37] T. Pridham, L. Lindenfelser, O. Shotwell, F. Stodola, R. Bendict, C. Foley, P. Jacks, W. Zaumeyer, W. Perston, J.W. Mitchell, *J. Phytopathol.* 46 (1956) 568.
- [38] R.M. Patil, *Acta Pol. Pharm.-Drug Res.* 64 (4) (2007) 345.
- [39] S. Shadomy, I. Epsinel, R. Cartwright, *Laboratory studies agent: susceptibility test and bio assay*, in: A. Lennette, W. Balows, H. Hausler, S. Shadomy (Eds.), *Manual of Clinical Microbiology*, fourth ed., Little Brown Co., Boston, 1985.
- [40] W.J. Geary, *Coord. Chem. Rev.* 7 (1971) 81–122.

- [41] K. Nakamoto, *Infrared Spectra of Inorganic and Coordination Compounds*, second ed., John Willy, New York, 1970.
- [42] L.-N. Zhu, M. Liang, Q.-L. Wang, W.-Z. Wang, D.-Z. Liao, Z.-H. Jiang, S.-P. Yan, P. Cheng, *J. Mol. Struct.* 657 (2003) 157–163.
- [43] F.A. Cotton, G. Wilkinson, *Advanced Inorganic Chemistry*, third ed., Wiley, London, 1972, p. 1145.
- [44] P.K. Dhara, S. Pramanik, T. Lu, M.G.B. Drew, P. Challopadyay, *Polyhedron* 23 (2004) 2457–2464.
- [45] B.S. Garg, D.N. Kumar, M. Sarbhai, *Spectrochim. Acta, A* 61 (2005) 141–147.
- [46] G. Cerchiaro, A.M. Ferreira, A.B. Teixeira, H.M. Magalhães, A.C. Cunha, V.F. Ferreira, L.S. Santos, M.N. Eberlin, J.M.S. Skakle, S.M. Wardell, J.L. Wardell, *Polyhedron* 25 (2006) 2055–2064.
- [47] B.J. Hathaway, D.E. Billing, *Coord. Chem. Rev.* 5 (1970) 143–207.
- [48] A.W. Coats, J.P. Redfern, *Nature* 201 (1964) 68–69.
- [49] H.H. Horowitz, G. Metzgar, *Anal. Chem.* 35 (1963) 1464–1468.
- [50] W.S. Lopes, C.R. Morais, A.G. de Souza, V.D. Leite, *J. Therm. Anal. Calorim.* 79 (2005) 343–347.
- [51] A. Despaigne, J. Silva, A. Carmo, O. Piro, E. Castellano, H. Beraldo, *J. Mol. Struct.* 920 (2009) 97.
- [52] F. Chen, Z. Xu, P. Xi, X. Liu, Z. Zeng, *Anal. Sci.* 25 (2009) 359–363.
- [53] S. Tabassum, A. Asim, F. Arjamand, M. Afzal, V. Bagchi, *Eur. J. Med. Chem.* 58 (2012) 308–316.
- [54] M. Baldini, M. Belicchi-Ferrari, F. Bisceglie, P. Dall'Aglio, G. Pelosi, S. Pinelli, P. Tarasconi, *Inorg. Chem.* 43 (2004) 7170–7179.
- [55] S. Tysøe, R. Morgan, A. Baker, T. Streckas, *J. Phys. Chem.* 97 (1993) 1707–1711.
- [56] S. Sarkar, A. Mondal, D. Chopra, J. Ribas, K. Rajak, *Eur. J. Inorg. Chem.* (2006) 3510–3516; J. Chen, X. Wang, Y. Shao, J. Zhu, Y. Zhu, Y. Li, Q. Xu, Z. Guo, *Inorg. Chem.* 46 (2007) 3306–3312.
- [57] A. Dimitrakopoulou, C. Dendrinou-Samara, A.A. Pantazaki, M. Alexiou, E. Nordlander, D.P. Kessissoglou, *J. Inorg. Biochem.* 102 (2008) 618–628.
- [58] S. Dhar, M. Nethaji, A. Chakravarty, *J. Inorg. Biochem.* 99 (2005) 805–812.
- [59] E. Chalkidou, F. Perdih, I. Turel, et al., *J. Inorg. Biochem.* 113 (2012) 55–65.
- [60] G. Li, K. Du, J. Wang, J. Liang, J. Kou, X. Hou, L. Ji, . Chao, *J. Inorg. Biochem.* 119 (2013) 43–53.
- [61] V. Uma, M. Kanthimathi, T. Weyhermuller, B. Nair, *J. Inorg. Biochem.* 99 (2005) 2299–2307.
- [62] J. Wu, L. Yuan, J. Wu, *J. Inorg. Biochem.* 99 (2005) 2211–2216.
- [63] B. Selvakumar, V. Rajendiran, P. Maheswari, H. Stoeckli-Evans, M. Palaniandavar, *J. Inorg. Biochem.* 100 (2006) 316–330.
- [64] S. Mukherjee, S. Chowdhury, A. Ghorai, U. Ghosh, H. Stoeckli-Evans, *Polyhedron* 51 (2013) 228.
- [65] R.M. Patil, *Acta Pol. Pharm.-Drug Res.* 64 (2007) 345–353.